Analysis of VHCF damage in a duplex stainless steel using hard X-ray diffraction techniques

Konstantin Istomin [a,*], Benjamin Dönges [b], Norbert Schell [c], Hans-Jürgen Christ [b], Ullrich Pietsch [a]

[a] Department of Physics, University of Siegen, Walter-Flex-Str. 3, D57072 Siegen, Germany
[b] Institute of Materials Engineering, Department of Mechanical Engineering, University of Siegen, Paul-Bonatz-Str. 9-11, D57076 Siegen, Germany
[c] Helmholtz-Zentrum Geesthacht Centre for Materials and Coastal Research, Max-Planck-Str. 1, D21502 Geesthach, Germany

ARTICLE INFO

ABSTRACT

Effects of very high cycle fatigue (VHCF) damage were investigated in an austenitic–ferritic duplex stainless steel using the hard X-ray diffraction technique applying a beam diameter in the order of the mean grain size. Diffraction patterns were collected using a large 2D detector as function of the position along the load axis as well as perpendicular to the load axis of hourglass-shaped ultrasonic fatigue specimens. Intensities, angular positions and widths of Bragg reflections from individual grains were studied as a function of load cycles and stress amplitudes. Whereas rocking curves (RC) of ferrite grains behave nearly unaffected by the cyclic load, a splitting of RCs of austenite grains was observed and is taken as an indication for the VHCF damage. The frequency of split RCs of austenite grains increases with the number of load cycles and is found to be a function of the local stress amplitude. The latter one can be modeled by means of the finite element method (FEM). Taken from the 2Θ angles of Bragg peaks the internal compressive lattice strain of ferrite and austenite grains is found to be released for low but increases again for high numbers of load cycles. The evolution of lattice strain and the frequency of split RCs of austenite grains correlate with the appearance of slip bands at the sample surface seen by scanning electron microscopy (SEM) in combination with electron channeling contrast imaging (ECCI) and in the bulk verified by transmission electron microscopy (TEM). Microcrack formation in ferrite grains is assumed originated by the high density of slip bands in austenite grains generated by very high cycle fatigue.

© 2014 Elsevier Ltd. All rights reserved.

1. Introduction

Austenitic–ferritic duplex steels are used for structural applications when high strength in combination with excellent corrosion resistance is required [1]. Many of these applications imply cyclic loading and hence, fatigue damage needs to be considered for dimensioning. Most design strategies make use of the fatigue-limit concept. Nowadays, the fatigue-limit concept is based on the idea that existing slip bands or microcracks are formed but blocked by microstructural barriers such as grain or phase boundaries. However, more recent research work has shown that metallic structures may fail far below the conventional fatigue limit even at very high numbers of cycles to failure [2,3]. Hence, it appears very doubtful, whether a true fatigue limit (corresponding to infinite fatigue life) can generally by assumed.

The interest in the behavior of materials at numbers of loading cycles beyond 10^7 results mainly from the demand of robust life prediction and damage evaluation assessment methodologies required for an increasing number of components. Although it is of common consensus that fatigue in the VHCF regime is dominated by crack initiation rather than crack growth, even for so-called run-out specimens traces of fatigue damage in the form of microcracks and/or slip band formation can be observed [4,5]. For the austenitic–ferritic duplex steel, slip band formation in the VHCF regime can be correlated with shear stress maxima deriving from stress concentrations due to elastic anisotropy and dislocation pile-ups [6].

In order to develop a better understanding of the nature of fatigue damage evolution under VHCF loading conditions, which are characterized by a macroscopically elastic behavior and a microscopically localized cyclic plasticity, not just microcracks have to be evaluated with regard to their propagation capabilities. Rather, microstructural changes have to be identified in order to shed light on those processes, which are responsible for the localized evolution of damage. This is done best by combining new sensible examination techniques which can provide both integral and local information on the effect of low-amplitude loading on the microstructural condition.

The present paper deals with the observation of local plasticity, fatigue damage, microstructural changes and strain evolution in an austenitic–ferritic duplex stainless steel in the VHCF regime. High-frequency fatigue testing in combination with SEM and TEM was applied. X-ray diffraction of hard X-ray was used to monitor the VHCF-induced alterations in individual grains of both phases. The results indicate that fatigue damage evolution during VHCF loading leads to a splitting of characteristic diffraction peaks of rocking curves (RC) of the austenitic phase only.

2. Materials and methods

The investigated duplex stainless steel X2CrNiMoN22-5-3 (German designation: 1.4462) with a two-phase microstructure consists of the austenitic γ-phase (fcc) and the ferritic α-phase (bcc) (Fig. 1). The heat treatment was carried out in such a way that the volume fraction of each phase is approximately 50 pct.

Symmetric push–pull fatigue experiments were carried out by means of an ultrasonic fatigue testing system [7] at about 20 kHz at room temperature in laboratory atmosphere. The testing system induces a sinusoidal mechanical stress wave into a fatigue sample at its resonance frequency. Resonance causes the required stress amplitude in the area of minimum cross section of the fatigue sample. The amplitude is kept constant by means of a control system. Heat generation of the investigated material during the fatigue tests requires a pulse–pause mode (100 ms/1200 ms) and an air-cooling system to restrict the temperature rise to maximum 5 °C. The pulse–pause mode causes an effective testing frequency of about 1.5 kHz, which enables the testing of very high numbers of load cycles in a reasonable time (e.g. 10^9 load cycles in about 7.5 days).

The crystallographic orientations and phase distributions were investigated by means of automated electron backscatter diffraction (EBSD) analysis. This data served for the calculation of Schmid factors and the determination of favorable slip systems. Dislocation arrangements in the bulk material of run-out samples (samples which endured 10^9 load cycles without fracture) were investigated by means of TEM examination of lamellae prepared by electrochemical jet polishing.

2.1. Samples preparation

The hourglass-shaped fatigue samples (Fig. 2b) were produced from cylindrical bars with a diameter of 25 mm by machining and subsequent grinding and electrolytically polishing. The
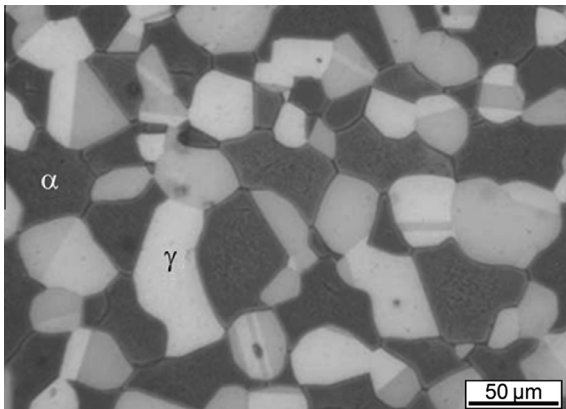

Fig. 1. Microstructure of the investigated duplex stainless steel containing austenite (γ, fcc, bright areas) and ferrite (α, bcc, dark areas) after heat treatment [8].

delivered material was hot rolled and solution annealed and showed a fine, lamellar microstructure with a volume fraction of 50 pct. of austenite and ferrite as well. This as-received condition was annealed at 1250 °C for 4 h, subsequently cooled down to 1050 °C within 3 h and finally quenched in water. This heat treatment was executed in order to simplify the experimental investigations by means of grain coarsening. The mean grain diameters after the annealing procedure were 33 μm for the austenite and 46 μm for the ferrite phase. The volume fraction of the two phases was maintained at 50% each.

2.2. Experimental set-up

The X-ray experiment was performed at high energy P07 beamline at PETRA III storage ring at DESY (Hamburg) using a photon energy of 87 keV and a micro beam with a diameter of about 50 μm and a fast read-out image plate 2D-detector (2048 × 2048 pixels) with the pixel size of 0.2 mm. The high photon energy (absorption length 2.5 mm in steel) allowed for probing the whole sample in transmission mode and the required size of the micro beam corresponded to the mean grain size. The experimental set-up is shown schematically in Fig. 2a. The vertical axis of the hourglass-shaped sample was aligned parallel to the rotation axis of the goniometer. The sample to detector distance was 1170 mm. The beam size was reduced to $50 \times 50\ \mu m^2$ using 2 pairs of slits and the samples were rocked around their axis of rotation (angle Ψ) in the range of ±2.0° with the step of 0.05°. The exposure time for each shot was 1 s. The diffracted beam was registered using the 2D-detector as the function of the rotation angle Ψ. Samples, which had been cyclically loaded up to different numbers of load cycles ($N_1 = 0$, $N_2 = 10^5$, $N_3 = 10^7$ and $N_4 = 10^9$) at an amplitude of 380 MPa were measured at the waist of the specimen. At the sample, which had experienced 10^9 load cycles, exposures were taken as function of the position along the load axis of the specimen (see sketch in Fig. 2).

3. Results

Due to random orientation of grains with respect to the incident beam, Debye–Scherrer like diffraction patterns appear at the detector where the ring diameters corresponds to different Bragg angles 4θ. A typical line profile of the diffraction intensity is shown in Fig. 3 obtained after integration of the ring intensity over an azimuth angle of 4°. It shows well resolved Bragg peaks which can be attributed to either ferrite or austenite structure. Because of the relative small number of grains fulfilling the Bragg condition at the same time, the Debye–Scherrer rings split into a large number of individual spots. By sorting 2θ each spot can be identified as either austenite or ferrite Bragg peak and indexed according to its radial position (Fig. 2a). Since most of the peaks are produced by a single grain, which satisfies the Bragg condition, the experiment allows for a single grain analysis.

The RC, i.e. the intensity distribution as function of the Bragg angle θ of a given grain, can be obtained by plotting the spot intensity from pattern taken at different rotation angle Ψ of the sample. Thus considering the Ewald's sphere [10] for the given experimental geometry, the best effective resolution in terms of the diffraction angle θ is obtained for those grains whose diffraction vector lies in the plane spanned by the incident beam and the normal to the detector plane. For these grains the scattering vector is nearly parallel to the vertical (load) axis and the angular resolution is in the order of the step widths used for rotation, to be $\Delta\Psi = 0.05°$. For all other orientations of the diffraction vector the resolution is larger than $\Delta\Psi$. By this reason the angular range for azimuthal integration was limited to 4° (see Fig. 3).
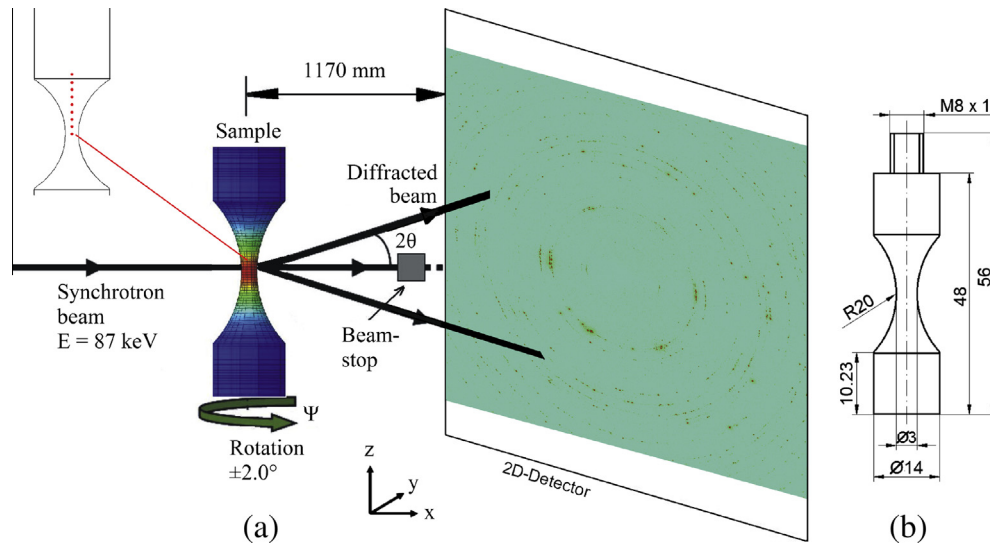
Fig. 2. (a) Experimental set-up (Beamline P07, side station). The measured spots along the vertical axis of the sample, which endured 10^9 load cycles without fracture, are shown in the upper-left corner and (b) drawing of an ultrasonic fatigue sample.
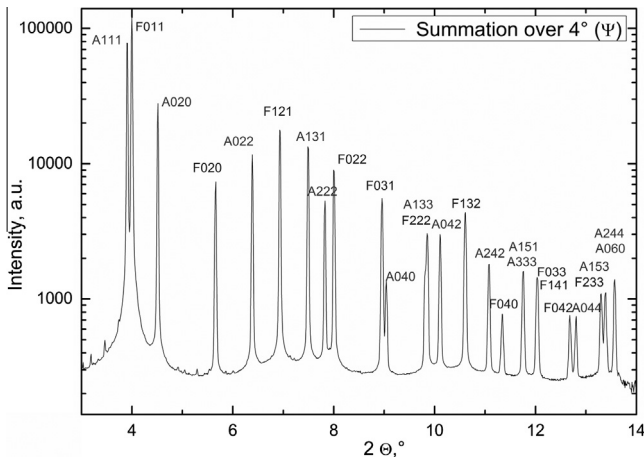

Fig. 3. Diffraction pattern (azimuthally integrated).

3.1. Splitting of austenite reflections

A large number of austenite of ferrite grains was analysed for four different samples with various degree of accumulated VHCF damage, with total numbers of grains varying from 51 to 169, depending on availability of respective grains fulfilling the Bragg condition for the given sample. It was found that the RCs of many austenite grains show two or more sub-peaks with splitting angle varying between 0.25° and 2.80°, which means that the respective grain was split into sub-grains caused by fatigue. At the same time the ferrite grains are rarely split and are less affected by fatigue (see examples in Fig. 4a and b).

Without quantification of the split amount, the splitting was further considered as indication of VHCF damage. Therefore, the fraction of split RCs was measured as the function of load cycles N_1 to N_4 in the centre of the specimen. Additionally the sample, which was fatigued until 10^9 load cycles (N_4), was investigated at 10 different points along the load axis and 5 points perpendicular to the load axis. Fig. 5a shows the fraction of split RCs of [1 3 1] austenite reflections as function of N_i (see box in Fig. 5a) and for sample N_4 as function of distance from the centre of the sample. The split grain fraction increases from about 15% to more than 30% for samples N_1 and N_2 and further up to a value of close to 40%

for samples N_3 and N_4. It appears that the fraction of such split RCs decreases in longitudinal (vertical) direction with distance from the sample centre, where the stress amplitude is the highest. At large distance it drops to a value comparable to the not prefatigued sample. Fig. 5b shows the behavior of sample N_4 in the radial direction. In this case, the split grain fraction increases with the distance from the centre towards the surface. The dashed lines show the courses of the amplitude of the von Mises stress, which were determined by means of finite element calculations.

Finite element calculations were executed by means of the commercial software ABAQUS. The material response was calculated in the framework of linear elasticity theory considering the elastic parameters Young's modulus $E = 197$ GPa and Poisson's ratio $v = 0.3$. The density was assumed to be $\rho = 7.85$ kg/m³). Quadratic hexagonal elements (C3D20R) were used for modeling. The mesh was refined in and near the testing cross section of the fatigue sample in order to obtain more accurate results. The resonance frequency of the sample was determined by means of a frequency analysis. To determine the von Mises stress distribution in the sample under resonance testing conditions, a base motion in direction of the sample load axis was applied at the restraint at one end of the sample at its resonance frequency. The other end of the sample had no boundary conditions.

3.2. Strain impact on peak broadening as function of load

Usually the impact of strain is probed by applying modified Williamson–Hall and Warren–Averbach procedures [9], i.e., plotting the full width at half maximum (FWHM) of austenite and ferrite reflections as function of $\tan \theta$ using line profile data as shown in Fig. 3. Unfortunate this method cannot be applied in this work because the grain size is in the order of the beam size and because not all grains are affected by fatigue.

Therefore we applied the method introduced by Mcirdi et al. [11] and studied the strain impact at single grains. In particular we determined the Bragg angle positions, 2θ, by azimuthally integrating of selected ferrite and austenite grains as function of N_i and determined the respective lattice parameters and their respective distribution among several dozens of individual grains of same phase. The results are shown in Fig. 6 for ferrite and austenite grains. Although the internal strain of all four samples is unknown, it turns out that for both grain types the lattice parameter of N_2 is
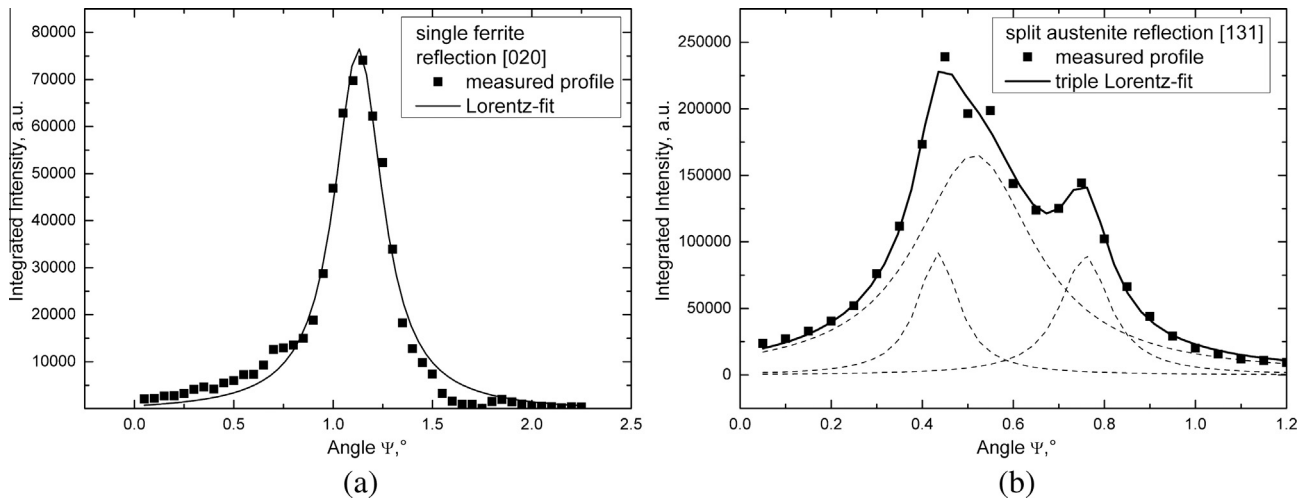
Fig. 4. (a) RC of a single ferrite reflection and (b) split RC of an austenite grain. Resulting fits are shown in solid line, while individual Lorentzian fits are shown in dashed lines.
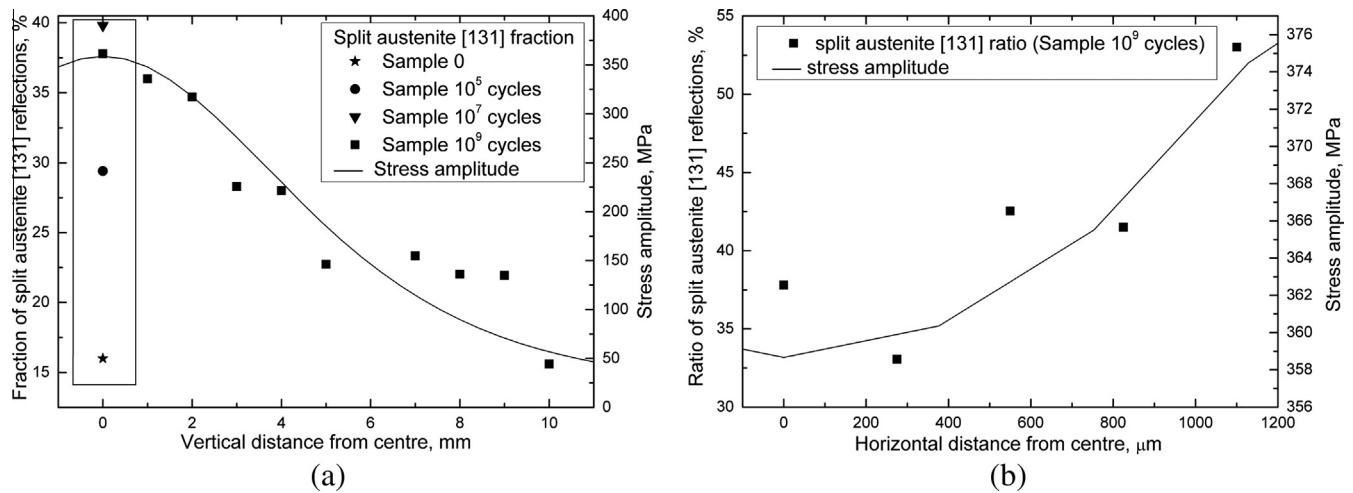

Fig. 5. (a) Fraction of split RCs of [131] austenite reflections as function of the vertical distance (solid squares) and comparison with other numbers of load cycles (other symbols inside the box at 0 mm) and (b) fraction of split RCs of [131] austenite reflections as function of the radial distance. Lines show the distributions of the amplitude of the von Mises stress (determined by FEM).
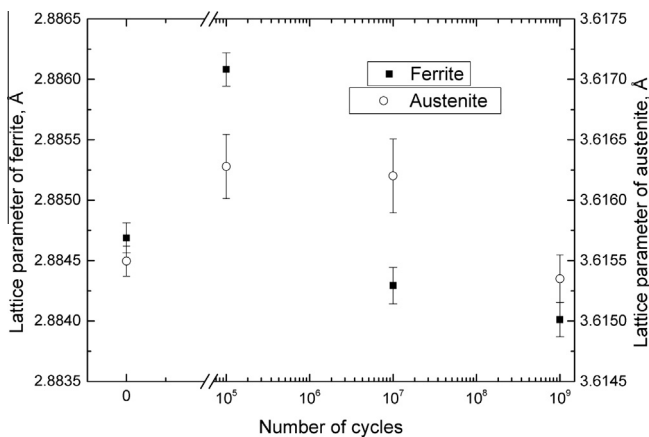

Fig. 6. Lattice parameters of ferrite and austenite grains as function of load cycles. Error bars are determined from the distribution of lattice parameters taken from several dozens of grains of same 2θ angle.

always larger as compared to N_1, but it decreases again for N_3 reaching for N_4 almost the same value as measured for N_1.

Considering that for the particular reflections under observation the N_1 is under compressive strain due to quenching the results indicate that the internal strain is partially released for low numbers but recreated for large numbers of load cycles. The strain release is approximately twice as large for ferrite as compared to austenite grains. On the other hand the distribution of strains is larger for austenite grains than for ferrite ones.

3.3. SEM and TEM inspection

The surfaces of the samples of the same series as used for X-ray examination were investigated by means of high resolution SEM (FEI Helios NanoLab 600) in combination with ECCI. Due to the relatively low load amplitudes applied, irreversible cyclic plastic deformation in form of slip band and slip trace generation was only observed in few austenite grains of the fatigued samples. By comparison, defect density in ferrite grains of these specimens was low (Fig. 7).

Several microcracks with a length of up to 80 μm, which were not able to grow further, have been observed in run-out samples. Comparing several of such features it was found that fatigue cracks frequently initiate transgranularly in ferrite grains, starting from
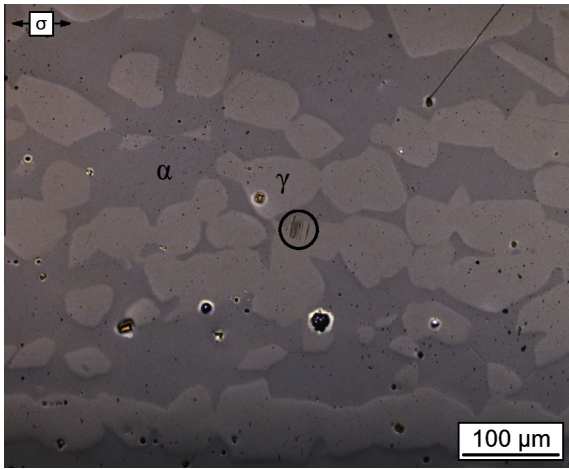
Fig. 7. Surface of a run-out sample with irreversible cyclic plastic deformation in few austenite grains (denoted by circle, $N = 10^9$, $\Delta\sigma/2 = 370$ MPa).

Fig. 9. Stacking faults and planar dislocation pile-ups against a phase boundary in a run-out sample ($N_4 = 10^9$, $\Delta\sigma/2 = 380$ MPa).

Fig. 10. Stacking faults and single dislocations in a run-out sample ($N_4 = 10^9$, $\Delta\sigma/2 = 380$ MPa), $z = [0\,1\,1]$.

intersection points between phase boundaries and austenite slip traces (Fig. 8). Stress intensifications at the tip of austenite slip bands can cause localized dislocation generation and motion in neighboring ferrite grains close to phase boundaries. The cyclic irreversible motion of dislocations on several parallel slip planes seems to determine the stage of fatigue crack initiation. The fatigue crack shown in Fig. 8 stopped at a length of about 11 μm without any visible influence of an obstacle (e.g. inclusion, grain or phase boundary) within a ferrite grain. A possible reason could be that the inhomogeneous stress field due to the anisotropic elasticity decreases stronger along the potential crack path than the stress field at the crack tip increases due to the increasing crack length. This may cause that the driving force (e.g. cyclic crack tip slide displacement, ΔCTSD) for further crack propagation vanishes.

Cyclic irreversible plastic deformation in form of slip band generation, which was observed by means of SEM in few austenite grains at the sample surface, was also observed in the bulk material by means of TEM (Hitachi H-8100, 200 kV) investigations at the depth of 0.6–0.7 mm, whereas the radius of the specimen in its center was 1.5 mm. Fig. 9 shows stacking faults and several slip bands in an austenite grain piling up against a phase boundary in a run-out sample, which was fatigued at 380 MPa. Another
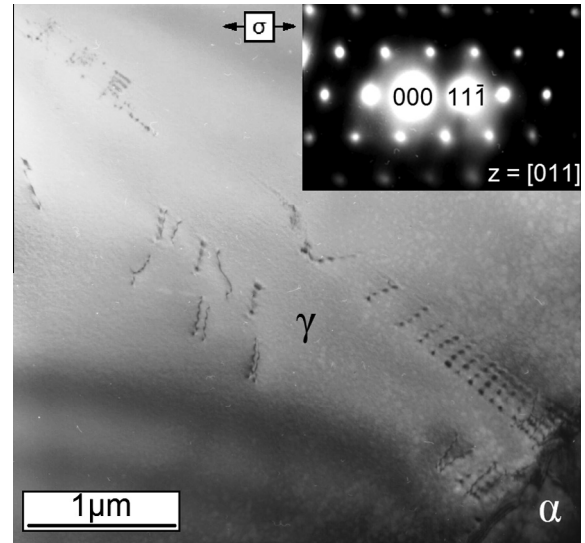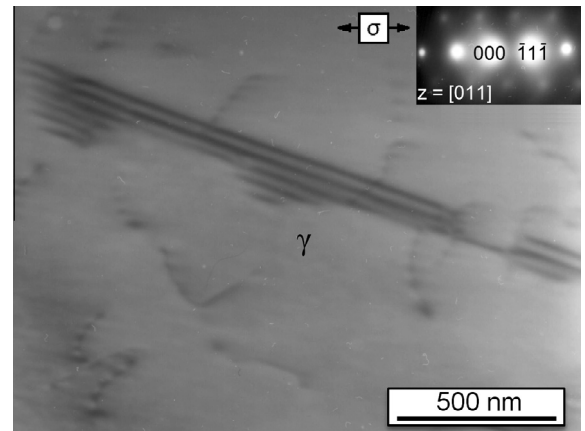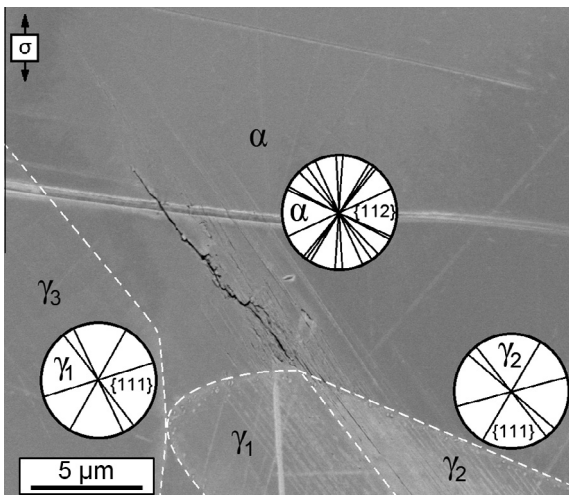

Fig. 8. Transgranular fatigue crack initiation in a ferrite grain due to slip band generation in an austenite grain ($N = 10^8$, $\Delta\sigma/2 = 380$ MPa), circles show possible slip traces.

austenite grain in this sample is presented in Fig. 10. An area of contiguous stacking faults and single, randomly distributed dislocations are shown.

4. Discussion

Using micro beam X-ray diffraction in transmission geometry we observed a systematic splitting of RCs of reflections of austenite grains as a function of the number of load cycles in austenitic–ferritic duplex stainless steel samples. The appearance of split RCs of austenite grains is correlated with the formation of slip bands causing grain substructures with mutual different orientation. Since the split angle is a function of the dislocation density and arrangement, it results from dislocation generation and gliding induced by the local shear stress amplitude [12]. Without quantifying the angular split amount, the frequency of split RCs of grains, i.e., the fraction of the austenite grains being split, increases as a function of the number of load cycles up to about 10^7 cycles and stays approximately unchanged up to 10^9 cycles. In addition we found a clear dependence of the split grain fraction as a function of the local stress amplitude. This behavior can be understood in

terms of linear elasticity and was modeled by means of FEM. Evaluating the lattice parameters at selected ferrite and austenite grains, the strain is partially released for low number of load cycles (sample N_2) but recreated for higher load cycles. That means that the internal strain becomes released due to the formation of more and more slip bands mainly in austenite grains. The respective bunching of dislocations form grain boundaries visible as split peaks in RCs up to 10^7 fatigue cycles. For higher number of stress cycles the additionally generated defects obviously are hindered to form new grain boundaries due to mutual hindrance which result in recreation of stress in both austenite and ferrite grains. The appearance of slip bands was verified by SEM at the surface and by TEM in the bulk of fatigued samples. On the other hand no major dislocation activity was found in the ferrite grains independent of the number of load cycles. This explains why no significant changes in X-ray RCs occurred for ferrite reflections. Crack formation was identified in several run-out samples. Here austenite grains with intense slip bands are forming cracks in neighboring ferrite grains. In some cases, these cracks stopped in the middle of the first grain without a visible influence of an obstacle (e.g. inclusion, grain or phase boundary). The mechanism of trans-granular fatigue crack formation in the ferritic phase resulting from high density slip band formation in austenite grains is assumed to be an important aspect for a detailed understanding of the VHCF behavior of duplex stainless steels. Methodically the proposed technique provides some challenges for the analysis of granular materials. In contrast to powder diffraction usually applied in material science to get averaging material parameters the method of micro beam X-ray diffraction allows for quasi single grain analysis. The appearance of split RCs found for a part of the austenite grains is correlated with the formation of slip bands revealed by SEM and TEM at selected grains also. The measured split angle can be attributed to a certain dislocation density generated by dislocation formation and gliding induced by the local shear stress amplitude [13]. The fraction of split RCs of grains varies non-systematically as a function of the azimuth angle measured from the load axis of the sample. This may give a hint of the effect of the Schmid factors of individual grains. Nevertheless, the fraction of split RCs of grains correlates with the local stress amplitude, e.g. along the load axis of the sample and in its radial direction. The results of electron microscopy investigations clearly support the assumption that the split RCs are caused by the dislocation arrangements because slip traces at the surface of fatigued samples (SEM) and slip bands in austenite grains (TEM) were found. It is proposed that the extent of this splitting can be used as a reasonable parameter quantifying fatigue damage.

5. Summary

In this paper we have investigated the influence of low-amplitude cyclic loading in the VHCF regime on the microstructure of duplex stainless steel. The appreciable changes are not uniform and limited to few austenite grains in particular after application of a small number of load cycles (up to 10^5): As a consequence of dislocation formation and glide, slip bands and subgrain boundaries are formed which results in a splitting of rocking curves of part of the austenitic grains. By means of hard X-ray diffraction technique applying a beam diameter in the order of the mean grain size, the split austenite grain fraction was clearly shown to increase with increasing local stress amplitude. Defect formation in a small number of grains causes a global strain release visible by increased lattice parameters of austenite and ferrite grains. The strain release in ferrite grains was found to be twice as large as compared to austenite ones. For more than 10^7 load cycles, more than 40% of austenite grains are affected. The high density of slip bands in these grains results in dislocation pile-ups against phase boundaries triggering transgranular fatigue crack initiation in adjacent ferrite grains, which finally may give rise to failure.

References

[1] Pohl M, Storz O. Sigma phase in duplex-stainless steels. Z Materi 2004;7:631–8.
[2] Sakai T. Review and prospects for current studies on very-high cycle fatigue of metallic materials for machine structural use. J Solid Mech Mater Eng 2009;3:425–39.
[3] Murakami Y, Endo M. Effects of defects, inclusions and inhomogeneities on fatigue strength. Inter J Fatigue 1994;16:163.
[4] Weidner A, Amberger D, Pyczak F, Schönbauer B, Stanzl-Tschegg S, Mughrab H. Fatigue damage in copper polycrystals subjected to ultrahigh-cycle fatigue below the PSB threshold. Inter J Fatigue 2010;32:872–8.
[5] Stanzl-Tschegg S, Schönbauer B. Mechanisms of strain localization, crack initiation and fracture of polycrystalline copper in the VHCF regime. Inter J Fatigue 2010;32:886–93.
[6] Marinelli M-C, Krupp U, Kübbeler M, Hereñú S, Alvarez-Armas I. The effect of the embrittlement on the fatigue limit and crack propagation in a duplex stainless steel during high cycle fatigue. Eng Fract Mech 2013. http://dx.doi.org/10.1016/j.engfracmech.2013.03.034.
[7] Mayer H. Fatigue crack growth and threshold measurements at very high frequencies. Inter Mater Rev 1999;44:1–35.
[8] Düber O, Untersuchungen zum Ausbreitungsverhalten mikrostrukturell kurzer Ermüdungsrisse in zweiphasigen metallischen Werkstoffen am Beispiel eines austenitisch-ferritischen Duplexstahls, Doctorate thesis, Universität Siegen, Fortschritt-Berichte VDI, Nr. 730, VDI-Verlag, Düsseldorf (2007).
[9] Ungár T, Gubicza J, Ribárik G, Borbély A. Crystallite size distribution and dislocation structure determined by diffraction profile analysis: principles and practical application to cubic and hexagonal crystals. J Appl Cryst 2001;34:298–310.
[10] Luger P. Modern X-ray analysis on single crystals. De Gruyter; 2011.
[11] Mcirdi L, Inal K, Lebrun JL. Analysis by x-ray diffraction of the mechanical behavior of austenitic and ferritic phases of a duplex stainless steel. Adv X-ray Anal 2000;42:397–406.
[12] Gottstein G. Physikalische Grundlagen der Materialkunde. Berlin: Springer Verlag, 3Aufl.; 2007. 246–251.
[13] Warren BE. X-ray diffraction. Dover Publications Inc.; 1990.